Experimental and numerical investigations on the dynamic response of turbine blades with tip pin dampers

# Experimental and numerical investigations on the dynamic response of turbine blades with tip pin dampers



2016 J. Phys.: Conf. Ser. 744 012131

(http://iopscience.iop.org/1742-6596/744/1/012131)

# Experimental and numerical investigations on the dynamic response of turbine blades with tip pin dampers

**S. Zucca[1], T. Berruti[1], L. Cosi[2]**

[1]Dept. of Mechanical and Aerospace Engineering, Politecnico di Torino
Corso Duca degli Abruzzi, 2410129 - Turin, Italy
[2]General Electric Company, GE Oil&Gas, Via Matteucci 2, Firenze, 50127, Italy
teresa.berruti@polito.it

**Abstract**. Friction dampers are used to reduce vibration amplitude of turbine blades. The dynamics of these assemblies (blades + dampers) is nonlinear and the analysis is challenging from both the experimental and the numerical point of view.
The study of the dynamics of blades with a tip damper is the aim of the present paper. The blades with axial-entry fir tree attachment carry a damper in a pocket between the blade covers. Pin dampers significantly affect the resonance frequency of the first blade bending mode and introduces non linearity due to friction contacts.
A test rig, made of two blades held in a fixture by an hydraulic press with one damper between the blades was used for the experimental activity. Three different types of dampers (cylindrical, asymmetrical, wedge) have been experimentally investigated and experiments have shown that asymmetrical damper performs better than the others.
The response of the blades with the asymmetrical damper was then simulated with a non linear code based on the Harmonic Balance Method (HBM). In the analysis, both the blade and the damper are modelled with the Finite Elements and then the matrices reduced with the Craig-Bampton Component Mode Synthesis (CB-CMS), while the periodical contact forces are modelled with state-of-the-art node-to-node contact elements. Numerical analysis has shown a strong influence of the actual extent of the contact area on the dynamics of the assembly. A model updating process was necessary. In the end, the numerical predictions match very well with the experimental curves.

## 1. Introduction

Due to the aggressive conditions during operation the forced vibrations of the blades in power turbines still represent one of the most common causes of failure. The design must prove robust enough to tolerate the occurrence of resonance under a wide operating range and with multiple engine order excitation. The different part of a turbine are connected together by interfaces. One of the challenge of the turbine designers is to correctly design these interfaces to provide adequate friction damping to the system.
In particular, existing joints may be optimized in order to exploit the damping contribution to limit the structure vibrations thanks to the dissipated energy at the contact (blade root joints [1], snubber [2] and shrouds [3]) or can be purposely added to the system (underplatform dampers [4], ring dampers [5]). The calculation of the nonlinear forced response of systems characterized by frictional damping cannot be performed by commercial FE solvers in a reasonable amount of time, and it requires the development of custom codes capable to compute the amount of frictional damping for a given excitation condition. Several authors ([6][7][8][9]) gave their contribution to take into account the actual stick-slip lift off states of the contact in order, to determine the real amount of change in the resonant frequency (stiffness

contribution) and in the resonant amplitude (damping contribution) due to the friction contact. Most of these papers deal with the modelling of underplatform dampers (UPD), which are metal devices compressed by the centrifugal force under the blade platforms which dissipate vibrations. In most of the cases the UPD is positioned under the blade platform that is close to the blade attachment. In this paper a blade tip damper is studied. Tip dampers are in principle similar to UPDs but they are placed at the blade tip and held in contact with the blade covers.
Due to their position, tip dampers are more challenging than UPDs, since they significantly change the mode shapes of the blades. Uncertainty in the actual contact conditions introduces a significant scatter in the resonance frequency and in the vibration amplitude.
First, in this work, tip dampers are experimentally investigated. Three different damper geometries (wedge-shaped, asymmetrical and cylindrical) are tested in order to identify the best performing damper, i.e. the damper that more reduces the vibration amplitude of the blades.
The architecture of the test rig is the same of test rigs used to investigate UPDs ([10]-[12]). Two blades are clamped in a fixture and then a damper is placed between them. Static load is provided to the damper by means of dead weight connected to the damper by a set of pulleys and steel wires.
Forced response is measured by a stepped sine approach. Excitation is provided by an electromagnetic shaker and the blades response is measured by accelerometers.
Then the forced response of the assembly (blades + damper) is investigated numerically. The nonlinear analysis in performed in the frequency domain with the Harmonic Balance Method (HBM) ([13]) and contact forces are modelled by node-to-node contact elements ([14]). In order to validate the numerical code, the numerical response curves are compared to the experiments corresponding to the best performing damper geometry (asymmetrical damper in this case).

## 2. The blades and dampers

The blades (Figure 1) have axial-entry fir tree attachment and they carry a damper in a pocket between the blades shrouds. Due the low length to chord ratio these blades are characterized by high stiffness and high natural frequencies even without the pin damper (the first bending frequency is higher than 1550 Hz). Being the damper located at the blade tip, it significantly affects the natural frequency of the first flexural mode and introduces non liberalities due to friction contacts.
Three different types of pin dampers (wedge, asymmetric, cylindrical) were tested (Figure 1).
The asymmetric damper is a combination of the other two: one side is curved like in the cylindrical damper, and one side is flat like in the wedge damper.
The forced response on the two blades with the damper between them was measured in order to determine the best performing damper which more effectively reduces the blades response.

## 3. Experimental set up

The test rig consists in a clamping system where an hydraulic press constraints the fixture holding the blades in the same relative position that they have in the disk (Figure 1). An electromagnetic shaker connected to one of the blade through a stinger produces the harmonic excitation of the blades ($F_e$).
The shaker is supported by four springs, linked to the rig structure. A force transducer positioned between the stinger and the blade measures the applied force, whose amplitude is kept constant during the test through a closed loop control system. The centrifugal force (Fc) on the damper is simulated by four cables equally spaced on the damper axis connected to plates carrying calibrated dead weights. Two accelerometers, one for each blade tip, measure the blade response.

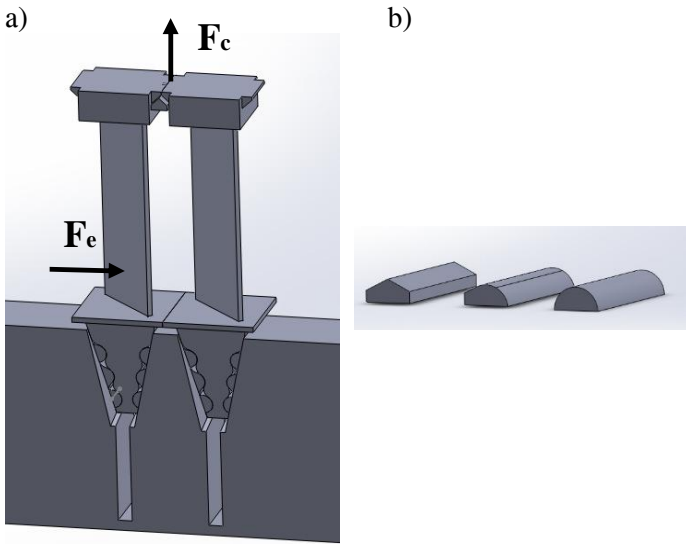


Figure 1 – a) Sketch of the blades during the test.
b) Geometry of the dampers

## 4. Test plan

The test consists in the measurement of the forced response of the blades with the damper during a stepped sine sweep. Each sweep corresponds to a different value of centrifugal force (Fc) on the damper and of excitation force (Fe).
The values of centrifugal forces included in the test matrix are 5 kg, 10 kg, 15 kg, 30 kg and 60 kg. Multiple levels of excitation force are measured in order to span a high number of Fc/Fe ratios corresponding to different contact states on the damper sides. The minimum excitation level depends on the signal/noise ratio, while the maximum value of Fe is limited by the capability of the acquisition system in controlling the force amplitude at resonance in closed loop.
For every level of centrifugal force, the following test procedure was used:
1) application of the dead weights on the loading plates (Fc);
2) excitation by the shaker (stepped sine) of the blade #1 at the different excitation force amplitude (Fe), at each frequency step the excitation force amplitude is controlled and kept constant at the target value (with a tolerance of about 1%);
3) disassembly of the damper from the blade, cleaning of the damper;
4) repetition of point 1) to 3) for three times.

## 5. Test results

The natural frequencies of the out-of-phase (OOP) and in-phase (IP) bending modes of the blades without tip dampers have been measured and their values are 1590 Hz and 1665 Hz respectively (Figure 2). It can be observed that a higher modal damping characterizes the IP vibration. The reason is that different mode shapes determine different friction damping at the blade root joint.

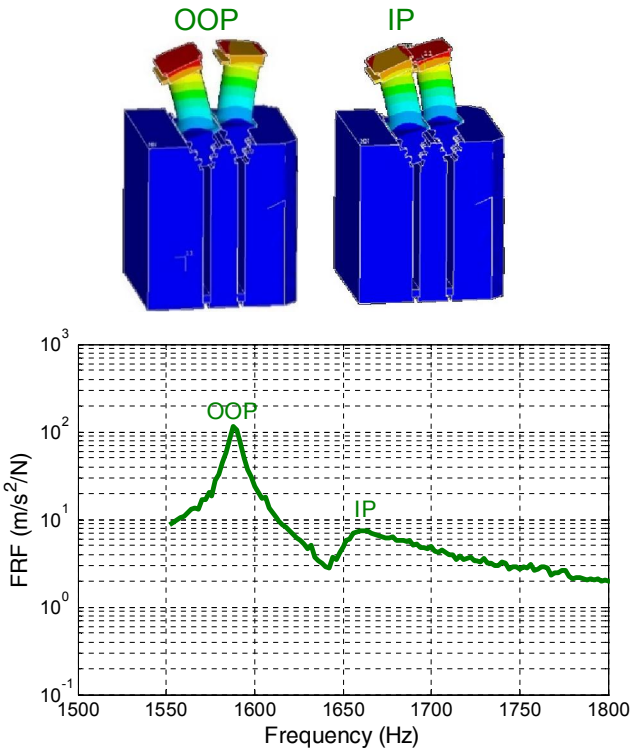


Figure 2 – Forced response of the assembly without tip dampers and corresponding numerical modal shapes.

As the damper is inserted in the blade slots, the IP dynamics of the blades does not change significantly, since the damper mostly rolls around its axes because of the relative motion of the blade platform ([11]). On the contrary, in case of OOP vibration the relative motion of the blade platforms produces relative displacements between the damper and the blades in the contact tangential and normal direction. As a result, a stiffening effect is observed and the resonance frequency moves to the range of 2500-3000 Hz. The forced response on the assembly with the damper was measured in order to determine the best performing damper.

The maximum amplitudes of the Frequency response function (FRF) are plotted in the form of "damper optimization curve" versus the ratio Fc/Fe (centrifugal force pulling the damper on excitation force amplitude). The curves corresponding to Fc = 60 kg are shown in Figure 3. The markers represent the average values error of the three repeated tests, the error bars represent the standard deviation of the measurements due to the repeatability.

The asymmetrical damper (red curves) produces the lower amplitude in the whole range for both the IP and OOP modes. This trend of the curves is confirmed also for the other values of centrifugal forces.

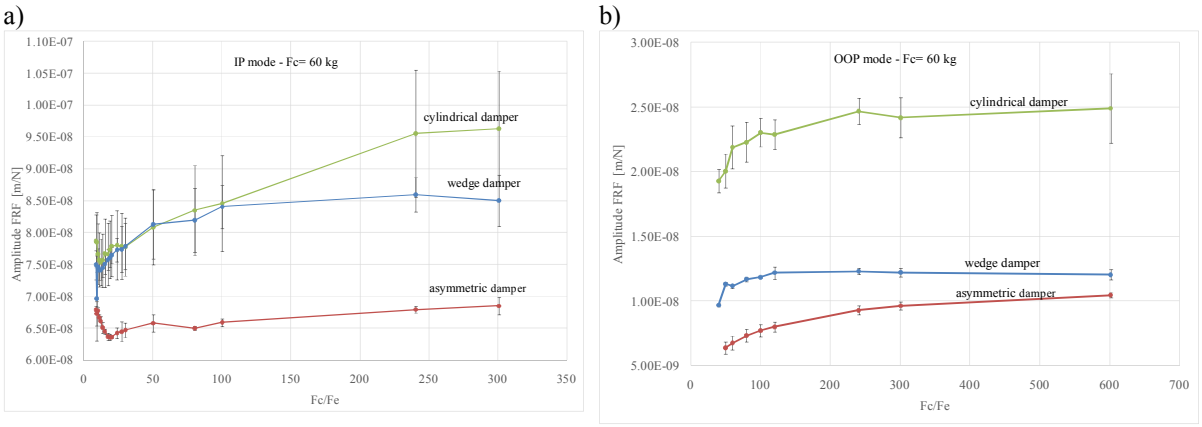


Figure 3 – Damper optimization curves in amplitude for Fc = 60 kg. a) IP mode b) OOP mode

## 6. The numerical simulation

The non-linear forced response of the assembly blades and damper is computed by a numerical code. Since the experiments have demonstrated the asymmetrical damper to be the most efficient one, only numerical analysis of the blade with the asymmetrical damper is performed, having the wedge and cylindrical dampers been discarded.

Two finite element (FE) models are developed: one of the two blades with the fixture, and one of the damper. Both models are then reduced by means of the Craig-Bampton ([15]) reduction method. The physical degrees of freedom (dofs) necessary to the analysis (e.g. contact, excitation and measurement dofs) are retained as master dofs in the reduced models, while the other dofs are modelled by superposition of linear normal modes with fixed interfaces. The reduced mass and stiffness matrices extracted by the FEM code are then used for the dynamic equations of blades and damper. These equations are described below.

### *6.1. Dynamic equations of the blades*

The non-linear dynamic equilibrium equations of the blades can be written as:

$$\mathbf{M}\cdot\ddot{\mathbf{Q}}(t)+\mathbf{C}\cdot\dot{\mathbf{Q}}(t)+\mathbf{K}\cdot\mathbf{Q}(t)=\mathbf{F}(t)+\mathbf{F}_{\mathbf{nl}}(t), \tag{1}$$

where **M**, **C** e **K** are the reduced matrices of mass, damping and stiffness of the two blades , **Q** is the vector of the nodal displacements and modal coordinates, **F** is the vector of the harmonic excitation force, $\mathbf{F}_{\mathbf{nl}}$ is the vector of the non linear contact forces due to the damper. The equation (1) is turned in frequency domain to be solved by means of the Harmonic Balance Method ([13]). The displacements and the contact forces are then expanded by Fourier analysis and truncated at their fundamental order:

$$\begin{aligned}\mathbf{Q}(t)&=\mathbf{Q}^{(0)}+\Re\left(\mathbf{Q}^{(1)}\cdot e^{i\cdot\omega\cdot t}\right)\\ \mathbf{F}_{nl}(t)&=\mathbf{F}_{nl}^{(0)}+\Re\left(\mathbf{F}_{nl}^{(1)}\cdot e^{i\cdot\omega\cdot t}\right)\end{aligned}, \tag{2}$$

By substituting (2) in (1) a new set of algebraic complex equations in frequency domain is obtained:

$$\begin{aligned}\mathbf{K}\cdot\mathbf{Q}^{(0)}&=\mathbf{F}_{\mathbf{nl}}{}^{(0)}\\ \mathbf{D}(\omega)\cdot\mathbf{Q}^{(1)}&=\mathbf{F}+\mathbf{F}_{\mathbf{nl}}{}^{(1)}\end{aligned}, \tag{3}$$

where $\mathbf{D}(\omega) = \mathbf{K} + i\omega\mathbf{C} - \omega^2\mathbf{M}$ is the dynamic matrix of the structure. The first equation (3) is the static equilibrium of the system, the second equation is the fundamental equation for the dynamic equilibrium of the structure.

*6.2. Dynamic equations of the damper*

As in the case of the blades, the equilibrium equations of the damper can be written as:

$$\mathbf{M_D} \cdot \ddot{\mathbf{Q}}_\mathbf{D}(t) + \mathbf{C_D} \cdot \dot{\mathbf{Q}}_\mathbf{D}(t) + \mathbf{K_D} \cdot \mathbf{Q_D}(t) = \mathbf{F_C} - \mathbf{F_{nl}}(t), \tag{4}$$

Where $\mathbf{M_D}$, $\mathbf{C_D}$ e $\mathbf{K_D}$ are the reduced matrices of mass, damping and stiffness of the damper, $\mathbf{Q_D}$ is the vector of the nodal displacements and modal coordinates, $\mathbf{F_C}$ is the centrifugal force on the damper. As in the case of the blades, after Fourier expansion and truncation at the fundamental order, a new set of algebraic complex equations is obtained in frequency domain:

$$\begin{aligned} \mathbf{K_D} \cdot \mathbf{Q_D}^{(0)} &= \mathbf{F_C} - \mathbf{F}_{\mathrm{nl}}^{(0)} \\ \mathbf{D_D}(\omega) \cdot \mathbf{Q_D}^{(1)} &= -\mathbf{F}_{\mathrm{nl}}^{(1)} \end{aligned}, \tag{5}$$

where $\mathbf{D_D}(\omega) = \mathbf{K_D} + i\omega\mathbf{C_D} - \omega^2\mathbf{M_D}$ is the dynamic matrix of the damper.

The contact forces between damper and platforms $\mathbf{F_{nl}}(t)$ are modelled by a set of 1D node-to-node contact elements ([14]). In order to model the 2D tangential forces, 2 mutually orthogonal elements are used at each contact pair. The contact element for each of the two tangential direction of each contact node is sketched in Figure 4 a). The periodic contact force $\mathbf{F_{nl}}(t)$ are then expanded in Fouried series and truncated at the order 0 and 1.

The two sets of non linear equations (3) and (5) are then solved by means of an iterative solver based on the Continuation Method ([16]).

Since the contact force at the blade roots due to the clamping device was not measurable, modelling the contacts between the blades and the fixture was pointless. The additional damping provided by the blade root joints was introduced in the model in terms of equivalent linear modal damping.

Contact parameters necessary for the contact force generation process are: static normal load, normal and tangential contact stiffness and friction coefficient. The static normal load is provided by the user as the output of a preliminary static analysis performed on the non-vibrating system. Contact stiffness are, in this case, computed by means of an analytical/numerical contact model based on the assumption of an ideal smooth contact of an elastic punch over an elastic infinite half-space ([17]). Friction coefficient must be provided by experimental tests performed on ad-hoc test rigs ([18]).

## 7. Contact Area and Contact Pairs

The contact surfaces between the blades and the damper are meshed with a regular and perfectly matching meshes in order to fulfill the requirement of perfectly matching contact pairs of the contact elements implemented to couple the bodies in contact to each other.

The whole flat damper side is theoretically in contact with the mating contact surface on the platform. Nevertheless, an a posteriori observation of the flat damper side after the experimental campaign (**Errore. L'origine riferimento non è stata trovata.** b)) has shown that wear is localized along a line at the lower edge of the flat surface.

As a consequence, only node pairs lying on that line have been activated during the nonlinear analysis, as shown in Figure 4 c).

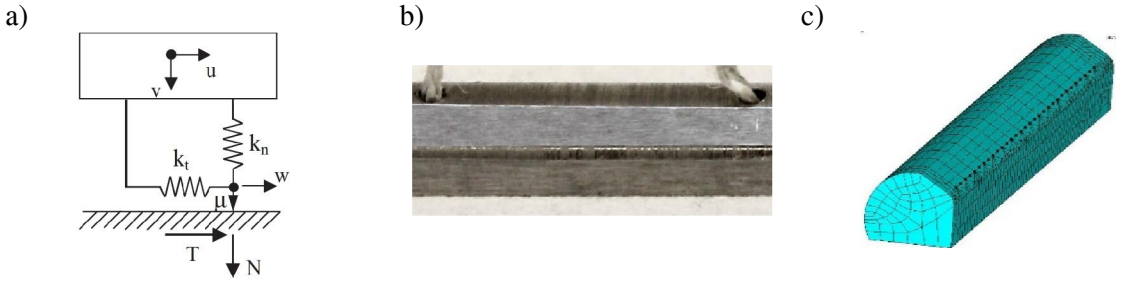


Figure 4 – a) Contact element. b) Wear areas at the damper edge. b) Damper model with contact nodes.

*7.1. Contact parameters*

A key point is the evaluation of the contact parameters: friction coefficient and contact stiffness (tangential and normal).

The value of the friction coefficient was measured through ad hoc experimental measurements as described in [18] In this case a value of 0.6 was measured at room temperature over a range of $5 \cdot 10^6$ cycles. The value of the contact stiffness is computed through a numerical contact model, developed in [17], and based on the principles of contact mechanics of a flat indenter with rounded edges, pressed onto an infinite half-space (Figure 5).

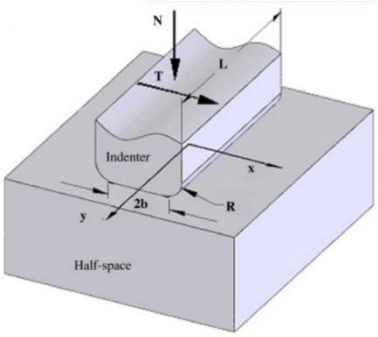


Figure 5– Flat indenter on an infinite half-space.

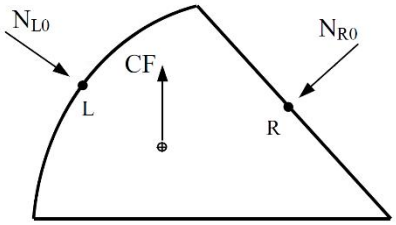


Figure 6– Static forces acting on the damper (frictionless contacts)

In case of the cylindrical contact, the extent of the flat area of the punch is null and the radius of the rounded edges of the punch are set equal to the cylinder radius.

In case of flat contact, the contact stiffness is computed by assuming a perfect flat contact (full rectangular contact area). The contact stiffness is then evenly distributed among the contact nodes. As a consequence, if only a subset of contact nodes is activated (**Errore. L'origine riferimento non è stata trovata.** c) in the previous section), the actual contact stiffness is proportional to the number of activated nodes.

To estimate the contact stiffness, a value of static normal force is necessary, since it affects the actual extent of the contact area of cylindrical contacts. The static normal forces on both damper sides are then computed by solving the static balance equation of the damper in case of frictionless contact (Figure 6).

In the end, a set of values of nodal contact stiffness have been computed for the cylindrical (Kt = 3.02E6 N/m; Kn = 3.32E6 N/m) and the flat (Kt = 0.94E6 N/m; Kn = 1.03E6 N/m) damper side.

## 8. Results and discussion

Experimental results corresponding to different levels of centrifugal forces of the damper were available. For the analysis, the OOP resonance of the first bending mode, with a centrifugal force Fc = 113 N, is selected (Figure 7), because a clear trend of the FRF curves versus the excitation level was observed. For the nonlinear forced response to be computed, an estimate of the linear damping of the structure is necessary. The values of damping ratio identified by means of hammer tests performed on the structure without the damper are not usable.

A part from the dampers, modelled in the numerical simulation, the other main damping source is represented by the blade root joints. As a consequence, the damping will depend on the excitation amplitude and on the mode shapes of the blades, strongly influenced by the damper and the contact state. The following strategy is here adopted: the FRF curve corresponding to the minimum excitation amplitude, controllable by the control system (Fe = 1 N in Fig. 7) is assumed to be the full-stick curve. Half-power method is then used to estimate a value of equivalent linear damping ratio $\zeta$ to be used in the nonlinear solver to build the linear damping matrix C.

In this way, a value of $\zeta = 0.022$ is estimated and hence used in all the simulations.

Firstly, the reference full-stick case (Fe = 1 N and Fc = 113 N) is computed and a resonance frequency of 3500 Hz is obtained, significantly larger than the experimental one (Figure 7).

This result highlights one of the main difficulties in the prediction of the response of structures with friction dampers: the additional stiffness provided by the damper, depending on the value of the contact stiffness and on the actual contact conditions of the damper surfaces. The case of tip dampers, as the one investigated in this work, is even more critical than underplatform dampers, due to the location of the damper (he blade tip) that increases the effect of the damper on the blade dynamics.

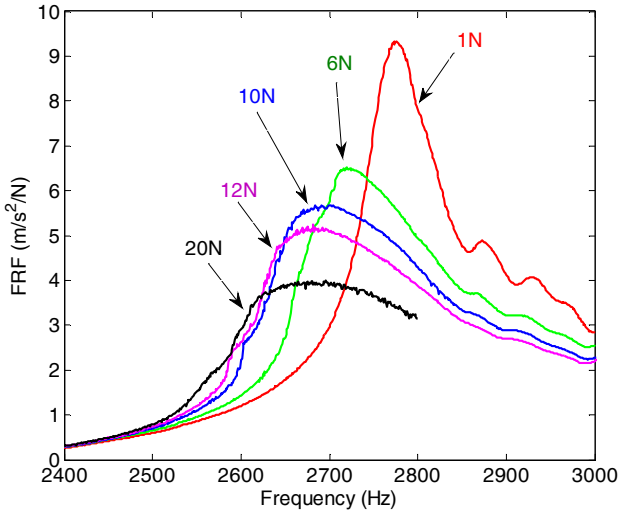


Figure 7– Average experimental FRFs at Fc = 113 N (3 repetitions).

In order to investigate the contact conditions over the damper length, the distribution of normal preload (product of the normal contact stiffness times the static normal relative displacement), obtained by a nonlinear static analysis is used.

It is observed that, although a multi-point loading system (Figure 8) is used to apply the 'centrifugal force' to the damper, a non uniform distribution of static normal load is obtained. In particular, the front

and the end of the damper are highly loaded (Figure 9), while the preload is lower at inner part and also detachment is predicted.

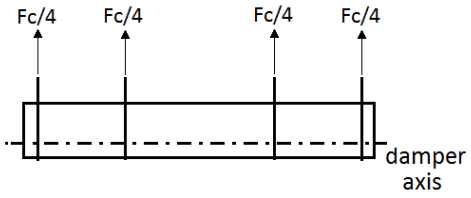


Figure 8 – Centrifugal force applied to the damper.

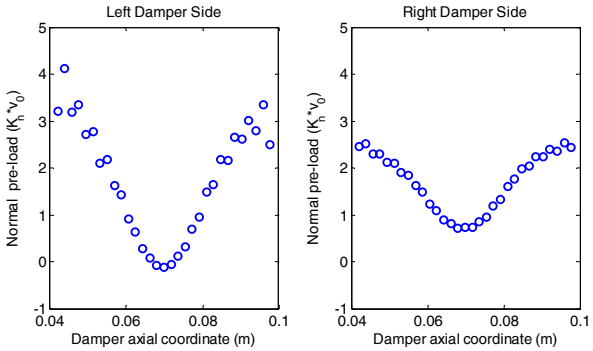


Figure 9 – Distribution of normal pre-loads on the damper sides.

On the basis of the results of the static analysis (Figure 9), the following tuning strategy is used: starting from the middle of the damper sides, contact pairs are progressively detached until the resonance frequency of the model at full-stick matches the resonance frequency of the reference experimental full-stick curve. The best match corresponds to 5 nodes in contact at one end and 4 nodes in contact at the other end of the damper, over a total number of contact pairs of 31.

The localization of the contact in the damper axial direction proves affects the system dynamics even more than the use of a single contact line over the flat damper side. Modelling the full contact on the flat damper side would give a resonance frequency at full-stick of around 3600 Hz, 3500 Hz are computed in case of full line contact, while around 2800 Hz in case of partial line contact.

After all the necessary parameters have been measured (friction coefficient), computed (contact stiffness) or estimated (damping ratio and number of contact nodes), the nonlinear forced response of the system at Fe = 20 N, 12 N, 10 N, 6 N and 1 N is computed.

For each forced response, 5 output nodes are selected on the excited blade (see Fig. 1), located in the area (75 mm$^2$) where the accelerometer was glued to the blade.

Results (Figure 10-Figure 14) are shown in descending order of the excitation level, as the contact tends from gross slip towards full-stick conditions. In each figure the full black lines represent the average (middle curve) and the average ± standard deviation (upper and lower curves), while the red dotted lines represent the maximum and the minimum response computed at the output nodes.

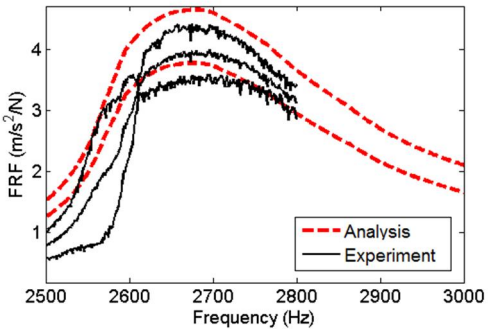


Figure 10 – FRF curves @ Fe = 20 N.

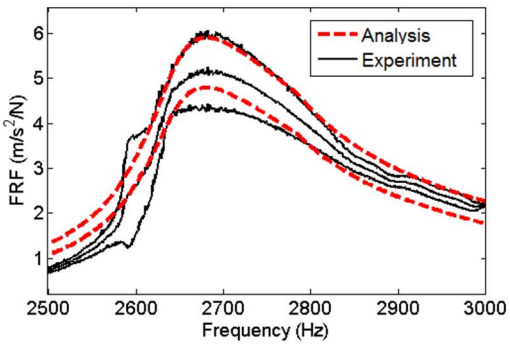


Figure 11 – FRF curves @ Fe = 12 N.

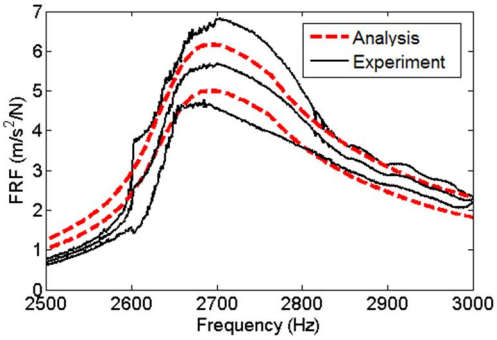


Figure 12 – FRF curves @ Fe = 10 N.

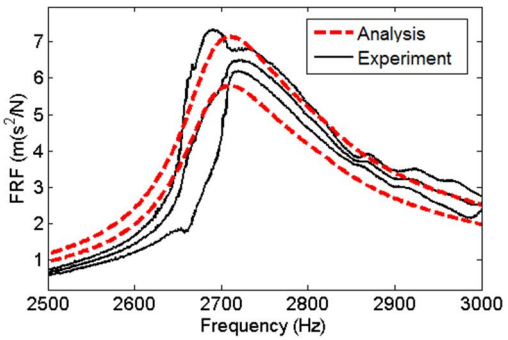


Figure 13 – FRF curves @ Fe = 6 N.

.

The numerical curves at Fe = 1 N (Figure 14) look more damped than the experimental ones. The reason is that the experimental curves have been used to compute the modal damping ratio of the full-stick case. During the simulation, the damper is not fully-stuck and therefore additional damping is provided by the sliding contacts.

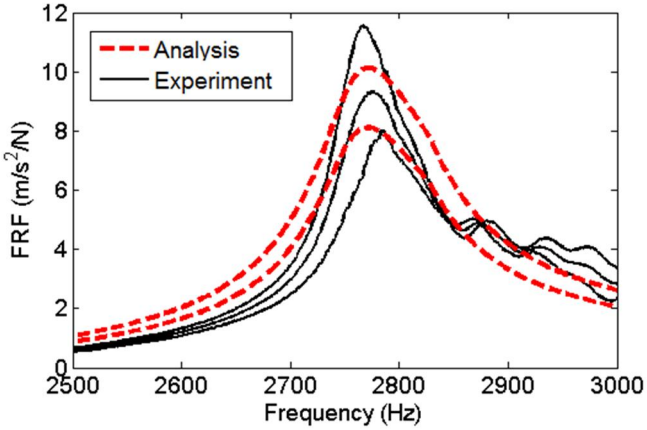


Figure 14 – FRF curves @ Fe = 1 N.

## 9. Conclusion

In this paper the dynamics of turbine blade with tip dampers has been investigated experimentally and numerically.

The experimental activity has been focused on the performances of different damper geometries and the asymmetrical damper (flat on one side and cylindrical on the other) has demonstrated better performances in reducing the response level of the blades around the 1st out-of-phase bending mode of the assembly.

A numerical analysis of the assembly with the asymmetrical damper has been then performed in order to predict the response levels at multiple excitation amplitudes.

The parameters necessary for the nonlinear forced response have been measured (friction coefficient and modal damping ratio) or computed (contact stiffness).

Preliminary numerical simulations have shown that the actual extent of the contact area strongly affects the dynamics of the system and a fine tuning of the contact nodes is necessary.
Nonlinear static analysis has shown that contact nodes at the axial ends of the damper are more heavily loaded and therefore they have been selected as contact nodes for the nonlinear forced response calculation.
In the end, the predicted forced response levels match very well the experimental curves at different excitation levels.

## 10. Acknowledgements

The authors are grateful to GE Oil & Gas for the permission to publish this work.

## 11. References

[1] Zucca, S., Firrone, C.M., Gola, M.M., 2011. Numerical assessment of friction damping at turbine blade root joints by simultaneous calculation of the static and dynamic contact loads. Nonlinear Dynamics 67, 1943–1955
[2] Pennacchi, P., Chatterton, S., Bachschmid, N., Pesatori, E., Turozzi, G., 2011. A model to study the reduction of turbine blade vibration using the snubbing mechanism. Mechanical Systems and Signal Processing 25, 1260–1275. doi:10.1016/j.ymssp.2010.10.006
[3] Siewert, C., Panning, L., Wallaschek, J., Richter, C., 2010. Multiharmonic Forced Response Analysis of a Turbine Blading Coupled by Nonlinear Contact Forces. Journal of Engineering for Gas Turbines and Power 132, 082501
[4] Firrone, C.M., Zucca, S., Gola, M.M., 2011. The effect of underplatform dampers on the forced response of bladed disks by a coupled static/dynamic harmonic balance method. International Journal of Non-Linear Mechanics 46, 363–375
[5] Laxalde, D., Thouverez, F., Lombard, J.-P., 2010. Forced Response Analysis of Integrally Bladed Disks With Friction Ring Dampers. Journal of Vibration and Acoustics 132, 011013. doi:10.1115/1.4000763
[6] E.P. Petrov, D.J. Ewins, Advanced modelling of underplatform friction dampers for analysis of bladed disk vibration, Journal of Turbomachinery 129 (1) (2007)
[7] L. Panning,WSextro, K. Popp, Spatial dynamics of tuned and mistuned bladed disks with cylindrical and wedge-shaped friction dampers, International Journal of Rotating Machinery 9 (3) (2003) 219–228
[8] C.M. Firrone, D. Botto, M.M. Gola, Modelling a friction damper: analysis of the experimental data And comparison with numerical results, in: Proceedings of the ESDA2006, Torino, Italy, ESDA2006-95605 (July 4–7, 2006).
[9] E.P. Petrov, Explicit finite element models of friction dampers in forced response analysis of bladed discs, ASME Turbo Expo 2007, May 14–17, Montreal, Canada, GT2007-27980 (2007
[10] Firrone, C.M., 2009. Measurement of the kinematics of two underplatform dampers with different geometry and comparison with numerical simulation. Journal of Sound and Vibration 323, 313–333. doi:10.1016/j.jsv.2008.12.019
[11] Y Sanliturk,, D. J Ewins., A. B. Stanbridge, Underplatform Dampers for Turbine Blades: Theoretical Modelling, Analysis and Comparison with Experimental Data, Proceedings of ASME Gas Turbine & Aeroengine Congress and Exhibition Indianapolis, 1999, ASME paper 99-GT-335.
[12] Jareland, M. H., “Experimental investigation of a platform damper with curved contact areas”, 2001, ASME 2001 Design Engineering Technical Conference, Pittsburgh
[13] Cardona, A., Coune, T., Lerusse, A., and Geradin, M., A Multiharmonic Method for Non-Linear Vibration Analysis,’ Int. J. Num. Methods Eng., 1994, vol. 37, pp. 1593–1608.
[14] Yang B.D., Chu M.L., Menq C.H., Stick–Slip–Separation Analysis and Non-Linear Stiffness and Damping Characterization of Friction Contacts Having Variable Normal Load, Journal of Sound and Vibrations, 1998, vol. 210 (4), pp. 461-481.

[15] Craig R.R., Bampton M.C.C., Coupling of Substructures for Dynamic Analyses, AIAA Journal, 1968, Vol. 6 (7), pp.1313-1319.
[16] Chan, T.F.C. & Keller, H.B. Arc-Length Continuation and Multigrid Techniques for Nonlinear Elliptic Eigenvalue Problems. SIAM Journal on Scientific and Statistical Computing, 1982, vol 3, p. 173.
[17] Allara M, A model for the characterization of friction contacts in turbine blades, Journal of Sound and Vibration, 2009, vol. 320, pp. 527-544.
[18] M. Lavella, D. Botto, M.M. Gola Design of a high-precision, flat-on-flat fretting test apparatus with high temperature capability Original Research Article Wear, Volume 302, Issues 1–2, 2013, pp.1073-1081.